UDC 620

S.V. Kovalyov, O.V. Ovchynnykov, K.M. Sukhyy, V.S. Yefanov, O.O. Kalinichenko, N.V. Koval'ova

PROPERTIES OF Zr–Ti–Nb AND Ti–Al–V ALLOYS

Ukrainian State University of Science and Technologies, Dnipro, Ukraine

This article is devoted to studying the properties of the new Zr–Ti–Nb alloy and comparing it with the well-known Ti–Al–V alloy (BT-6, Grade 5 analog). The properties were analyzed through chemical composition determination and corrosion resistance assessment. The Zr–Ti–Nb alloy does not contain the toxic impurities present in the Ti–Al–V alloy, specifically aluminum and vanadium. Structural studies were conducted to identify the phases (X-ray diffraction analysis) and their composition using scanning electron microscopy. The microstructure and phase composition of the Zr–Ti–Nb alloy indicated a uniform distribution of elements throughout the alloy. The wetting angle of the Zr–Ti–Nb alloy with an oxide layer is significantly smaller than that of the Ti–Al–V alloy, suggesting greater hydrophilicity. Physical research methods included determining density, reflectivity, and electrical conductivity. Mechanical properties were examined by determining the elastic modulus, strength limit, yield strength, longitudinal elongation, transverse contraction, and microhardness. Notably, the elastic modulus of the Zr–Ti–Nb alloy is 26.4 GPa, similar to that of cortical bone, in contrast to the Ti–Al–V alloy, which has an elastic modulus of 110–140 GPa. The obtained data indicate that the superior chemical and mechanical properties of the Zr–Ti–Nb alloy make it suitable for medical applications.

Keywords: biomedical alloy, Zr–Ti–Nb, Ti–Al–V, corrosion, wettability, chemical, structural, and mechanical properties.

DOI: 10.32434/0321-4095-2024-157-6-30-39

Introduction

The modern world and technologies that are rapidly developing in the 21st century require materials with properties that could not be predicted a few decades ago and especially, necessary materials with a set of certain properties at the same time. As an example, it is possible to cite biomaterials for the medical field [1–12], as well as a large number of technological materials [13,14].

Biomaterials used for the manufacture of implants in the field of orthopedics, dental implantology and cranioplastic surgery must have a whole set of the following characteristics: good biocompatibility, good osseointegration properties, high wear resistance and corrosion resistance in biological environments, as well as excellent mechanical properties and good biomechanical compatibility [1–3].

The biomechanical compatibility strongly depends on the value of the elastic modulus of the implant material, which is used to construct the bone and should preferably have the same elastic modulus as the bone itself [4]. Studies have shown that this will minimize atrophy of bone tissue due to the stress-shielding effect, and increase the service life of the implant [5]. Many studies are devoted to the search for new strong biocompatible materials with a low value of the elastic modulus in order to expand the possibilities of the field of modern implantology, in particular, to increase the service life of implants [6]. Due to high strength, corrosion resistance, excellent biocompatibility, and relatively low modulus of elasticity compared to other materials, titanium alloys

are the most common for the manufacture of implants [7].

Commercially pure titanium and the Ti–6Al–4V alloy are widely used in the field of modern implantology [8]. These materials have a modulus of elasticity of 105–115 GPa, which exceeds the elastic modulus of cortical bone, which is equal to 15–30 GPa [9]. In addition, the Ti–6Al–4V alloy contains toxic elements Al and V in its composition, the release of which in the biofluids of the body can lead to health problems in the long term [10]. Therefore, the task of manufacturing new biocompatible alloys with lower elastic modulus values, studying their properties, and improving the technology of obtaining the alloys is still relevant [11].

Mishchenko et al. [12] have developed a new biocompatible Zr–Ti–Nb alloy with a chemical composition of 59.57 wt.% Zr, 19.02 wt.% Ti, 21.41 wt.% Nb, and the alloy elastic modulus of 27.27 GPa, which indicates the possibility of using this alloy as a biomedical material for the manufacture of implants. The authors have also increased the economic efficiency of the alloy manufacturing technology.

The purposes of our work are as follows:

1) determination of the chemical, physical, mechanical properties and structure of the new Zr–Nb–Ti alloy;

2) comparison of the properties of the Zr–Nb–Ti alloy with those of the commonly used Ti–6Al–4V alloy;

3) development of recommendations on the use of the Zr–Nb–Ti alloy as a biomaterial.

Experimental

Materials

The Zr–Ti–Nb alloy was produced according to the method described elsewhere [12]. Grade 5 alloy (Ti–6Al–4V) was purchased from Zaporizhzhia Titanium&Magnesium Combine Ltd. (Zaporizhzhia, Ukraine).

Chemical composition

The chemical composition of the alloys was investigated by X-ray fluorescence analysis using the EXPERT 4L express analyzer.

X-ray phase analysis

The X-ray diffraction method was used to characterize the phase composition and structural parameters of both alloys. X-ray diffractograms were taken on a standard DRON-3 diffractometer with Bragg-Brentano geometry and filtered Co-Kα radiation. Data were obtained in the 2θ range from 20^0 to 130^0, with a step of 0.1^0 and a counting time of 5 seconds per step.

Scanning electron microscopy

The structure and composition, as well as the number and location of the main alloying elements, were evaluated using a Tescan Mira 3 MLU scanning microscope additionally equipped with an Oxford X-Max 80 mm^2 energy dispersive spectrometer, which additionally allows determining the elemental and quantitative composition. The research was conducted at an accelerating voltage of 15 kV and a diameter of the electron probe of 4 nm, the diameter of the X-ray excitation zone being about 2 μm. In addition, images of the surface of the Zr–Ti–Nb alloy sample after rupture were obtained using this method.

Wettability

The wettability was determined by measuring the edge angle using the optical microscopy method.

Corrosion resistance of alloys

Corrosion resistance was evaluated by analyzing the corrosion diagrams obtained for the alloys. The diagrams were obtained using a PI-50-1 potentiostat and a PR-8 programmer in an ordinary three-electrode cell. The reference electrode was a silver chloride electrode filled with a saturated KCl solution. The tests were carried out in a solution of 0.9 wt.% NaCl at a potential scan rate of 0.001 V/s.

Physical properties

Density was measured by dividing the weight of the sample by its volume. The volume was measured in two ways: direct measurement of the volume of a cylindrical sample and the method of displacement of water volume. The error of determining the density did not exceed 10%.

The reflectivity was determined using a FB-2 photoflash meter, where a silver mirror was used as a standard, the reflectivity of which was taken as 100%.

The electrical conductivity of alloys was measured by using a specially developed scheme for measuring the electrical conductivity of metals.

Mechanical properties of alloys

The mechanical properties of the alloys were studied using a P-5 breaking machine. Samples in the form of a «dumbbell» for a tearing machine were produced in accordance with the Ukrainian state standard DSTU ISO 6892-1:2019 by electrical erosion cutting of a cylindrical billet from an ingot and subsequent turning. To determine the mechanical properties, the following parameters were studied: tensile strength (σ_B, MPa), yield strength ($\sigma_{0.2}$, MPa), modulus of elasticity of the 1st kind (Young's modulus) (E, GPa), longitudinal elongation (δ, %), transverse narrowing (ψ, %). The measurement error did not exceed 10%. The hardness was measured using a

Vickers Hardness Tester (432SVD) of the Wolpert Group company. Microhardness was measured using PMT-3 microhardness tester. Microhardness values were obtained by determining the average value of at least five impresses along the surface for each alloy sample.

Statistics

Three samples were used for each measurement method. Statistical significance was accepted at a confidence level of 90% ($p<0.1$).

Results and discussion

Chemical composition of alloys

The elemental composition of alloys is given in Table 1, according to which the Zr–Ti–Nb alloy contains only the main components and iron impurities. In contrast, the Ti–Al–V alloy has, in addition to the main components, impurities of other elements that make up more than 1%. However, both alloys have the composition declared by the manufacturer.

Phase composition

The results of the phase analysis show that the Zr and Nb phases predominate in the samples of the Zr–Ti–Nb alloy (Fig. 1,a). There are Ti and $NbTi_4$ phases in the amount of up to 2%. No other phases were detected or their content is less than 1%.

Phase analysis of the Ti–Al–V alloy (Fig. 1,b) indicates that titanium predominates in crystalline samples. However, Al_5Ti_3 and $AlTi_2$ alloys are present. The unknown phase is also detected (about 2%), probably including vanadium.

Scanning electron microscopy

SEM-images of the surface of Zr–Ti–Nb alloy grinds obtained at different magnifications are shown in Fig. 2, a,c,e.

SEM analysis indicates a uniform distribution of Zr, Nb and Ti in the alloy. Three zones are distinguished on the surface of the samples: the «main» zone (the largest area, marked in Fig. 3,a as spectrum 2), the second «gray» zone (marked in Fig. 3,a as spectrum 1) and «black» zone (marked in Fig. 3,a as spectrum 3).

According to the data of elemental analysis, the «main» zone consists of alloy components found in the following contents (wt.%): titanium 16, zirconium 63, and niobium 21. The «gray» zone (approximately 15%) has the following composition (wt.%): titanium 20, zirconium 74, and niobium 6. The «black» zone (approximately 17%) has the following composition (wt.%): titanium 14, zirconium 65, and niobium 21. According to the analysis results, the second zone has a reduced content of niobium and an increased content of zirconium. However, the zones are located evenly along the surface and this should not affect the mechanical properties.

In the SEM images of the surface of Ti–Al–V alloy grinds (Fig. 2,b,d,f), two zones are highlighted: the «gray» zone, which has the largest area (Fig. 3,b marked as spectrum 2) and the second «white» zone (Fig. 3,b marked as spectrum 1). According to the

Table 1

Chemical composition of alloys

Alloy	Element content, wt.%										
	Ti	Zr	Nb	Fe	Al	V	Si	S	Cr	Ni	Cu
Zr–Ti–Nb	17.39	64.28	18.1	0.23	–	–	–	–	–	–	–
Ti–Al–V	88.5	–	–	0.5	6.43	3.94	0.1	0.05	0.25	0.19	0.03

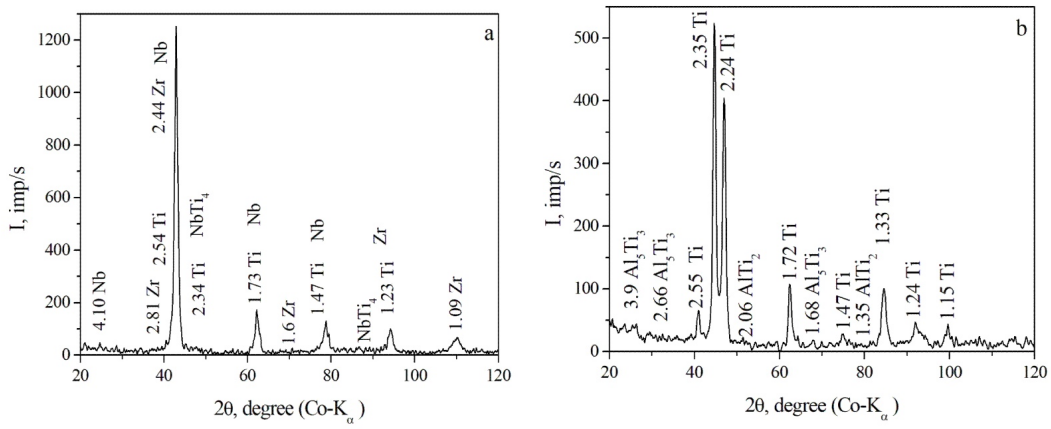

Fig. 1. XRD patterns of alloys under study: a – Zr–Ti–Nb; and b – Ti–Al–V

results of chemical analysis, the «gray» zone consists of the following alloy components (wt.%): aluminum 7.36, titanium 89.56, and vanadium 3.08, while the «white» zone (approximately 25%) has the following composition (wt.%): aluminum 3.89, titanium 79.79, and vanadium 16.23. According to the analysis of the Ti–Al–V alloy, the second zone has a reduced content of aluminum and titanium and an increased content of vanadium. In the case of the Ti–Al–V alloy, in contrast to the Zr–Ti–Nb alloy, the zones are not located evenly along the surface. This may worsen the mechanical properties of the Ti-Al-V alloy.

Wettability

Wettability is one of the characteristics of the biomaterial's surface, which affects the process of implant osseointegration. It follows from literature that more hydrophilic surfaces enhances the osseointegration process. Studies have shown that the surface energy of biomaterials strongly influences the initial cell attachment and spreading of osteoblastic cells on the biomaterial surfaces [1].

The wetting angle of the alloys was measured in two ways. In the first way, the surface of the alloy samples was not finished, and there was an oxide layer on the surface. In the second way, the surface of the samples was mechanically treated with 200 grade sandpaper to remove the oxide layer from the sample's surface. The photographs (Fig. 4) show almost the same strong hydrophobicity of the metal alloys that underwent preliminary treatment to remove the oxide film from the surface (Fig. 4, c and d). The wetting angle was $104^0 36'$ and $102^0 06'$ for the Zr–Ti–Nb and Ti–Al–V alloys, respectively. For alloys covered with an oxide layer, which were not previously finished (Fig. 4, a and b), the wetting angle was $45^0 18'$ and 64^0 for the Zr–Ti–Nb and Ti–Al–V alloys, respectively. The presence of an oxide film on alloys leads to a sharp change in their surface properties from hydrophobic to hydrophilic. It should be noted that Zr–Ti–Nb with an oxide film exhibits better hydrophilic properties than Ti–Al–V, which can affect the improvement of the osseointegration process. Table 2 shows the values of the measured wetting angles and the calculated data for the work of adhesion [1].

Electrochemical corrosion

The polarization curves were recorded for both alloys by scanning the electrode potential from open circuit potential to the anodic and cathodic regions with a sweep rate of 0.001 V/s (Fig. 5). There are three peaks in the potential range of −0.4 V to 0 V on the anodic curve registered for the Zr–Ti–Nb alloy. The first peak at a potential of −0.128 V probably

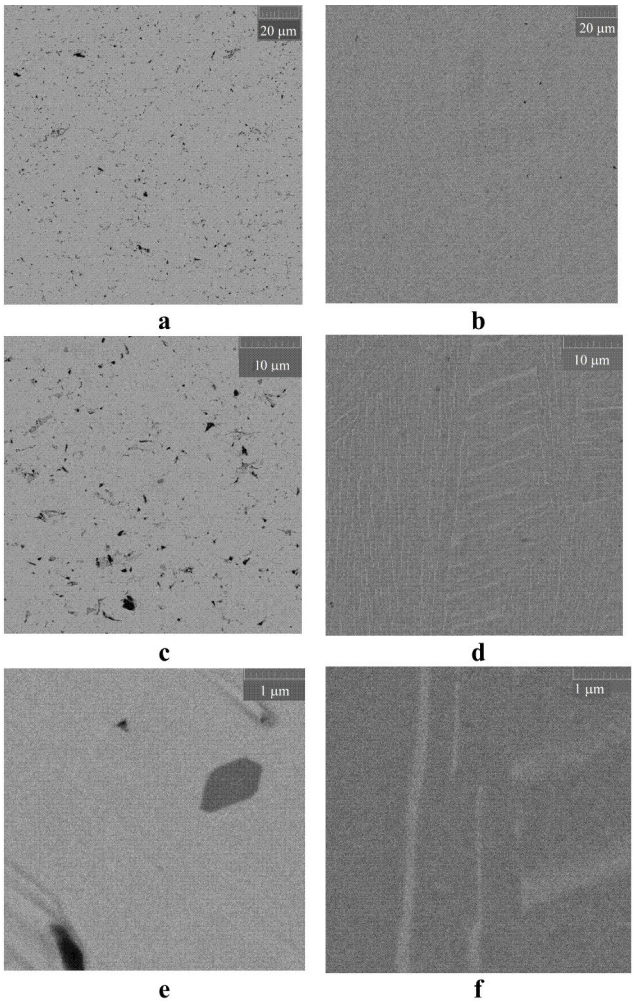

Fig. 2. SEM images of the surface of alloy samples obtained by scanning electron microscopy at different magnification: a, c, e – Zr–Ti–Nb; and b, d, f – Ti–Al–V

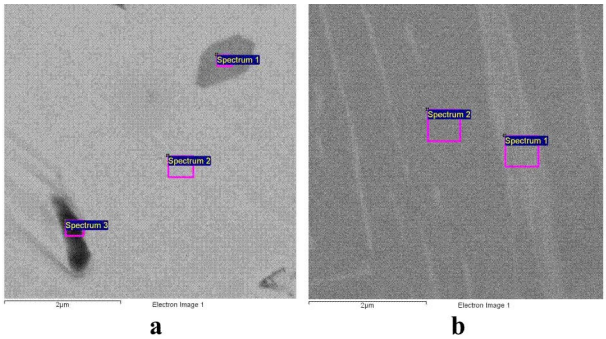

Fig. 3. SEM images of the surface of alloy samples obtained by scanning electron microscopy for the alloys: a – Zr–Ti–Nb; and b – Ti–Al–V

[1] Work of adhesion was calculated using the Young-Dupre equation.

corresponds to the oxidation of zirconium. The second peak at a potential of −0.073 V can be attributed to the oxidation of niobium. The third current peak at a potential of −0.015 V can be assigned to the oxidation of titanium. On the anodic curve for the Ti−Al−V alloy, only one current peak is observed at a potential of −0.015 V, which corresponds to the oxidation of titanium. At potentials above +0.075 V both alloys are passivated. Based on the obtained data, it is possible to recommend the following anodic treatment: polarization of alloy materials at potentials higher than +0.1 V in order to obtain a passive film on the surface and protect it against destruction.

Table 2

Wetting angle and work of adhesion

Alloy	Wetting angle (θ)	Work of adhesion (W), mJ/m^2
Zr–Ti–Nb with oxide film	45^{0}18'	124.3
Zr–Ti–Nb without oxide film	104^{0}36'	54.6
Ti–Al–V with oxide film	64^0	105
Ti–Al–V without oxide film	102^{0}06'	57.7

A comparison of the corrosion properties of alloys is shown in Fig. 6. Dependences are presented in the form of the decimal logarithm of the current density vs. the electrode potential to determine the stationary corrosion potential and corrosion current density for both alloys. The corrosion current is $3.16 \cdot 10^{-7}$ A/cm^2 and $7.11 \cdot 10^{-7}$ A/cm^2 for the Zr−Ti−Nb and Ti−Al−V alloys, respectively (Table 3). The corrosion potential (open circuit potential) in a solution of 0.9 wt.% NaCl is E_{cor}=−0.45 V and E_{cor}=−0.288 V for the Zr−Ti−Nb and Ti−Al−V alloy alloys, respectively. The corrosion current density for the Zr−Ti−Nb alloy is less important, but the Ti−Al−V alloy has a corrosion potential with a much more positive value (by 160 mV). This indicates higher corrosion resistance of the Ti−Al−V alloy. However, the above-mentioned anodic treatment is likely to be able to significantly improve the corrosion resistance of the materials in question.

Table 3

Corrosion properties of alloys

Alloy	Corrosion current, A/cm^2	Corrosion potential, V
Zr–Ti–Nb	$3.16 \cdot 10^{-7}$	–0.450
Ti–Al–V	$7.11 \cdot 10^{-7}$	–0.288

Physical properties

The study of physical properties was carried out by determining the density, reflectivity and electrical conductivity. The research data are given in Table 4. The density of the Zr−Ti−Nb alloy is 34% greater than that of the Ti−Al−V alloy, i.e. the Zr-Ti-Nb alloy products will have a greater weight compared to the Ti−Al−V alloy products of the same size. The reflectivity of the metal surface does not differ significantly, but it is somewhat higher for the Zr−Ti−Nb alloy. The electrical conductivity of the Zr−Ti−Nb alloy is greater than the electrical conductivity of Ti−Al−V, but this difference is not significant.

Mechanical properties

The tensile diagram of the Zr−Ti−Nb alloy sample is shown in Fig. 7. The curve has some

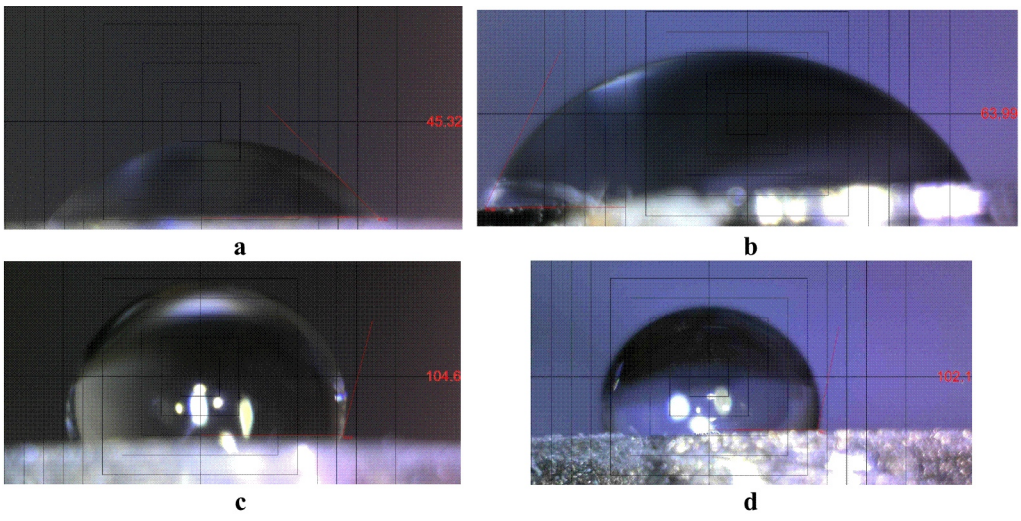

Fig. 4. Photographs of water drops on the surface of alloys: a and c − Zr−Ti−Nb; b and d − Ti−Al−V) to determine the wetting angle. a and b − drops on the surface of materials with an oxide film; c and d − drops on the surface of clean alloys

characteristic sections: linear region (up to stresses of about 510 MPa), the yield plateau of the alloy material at 530 MPa, and the strength limit (631 MPa). The value of the elastic modulus for the Zr–Ti–Nb alloy, was determined by analyzing the curve in Fig. 7, it is equal to 26.44 GPa (Table 5). This value coincides with the modulus of elasticity of cortical bone, which has a value of 15–30 GPa [9]. The summarized values of the mechanical characteristics of the alloys are given in the Table 5.

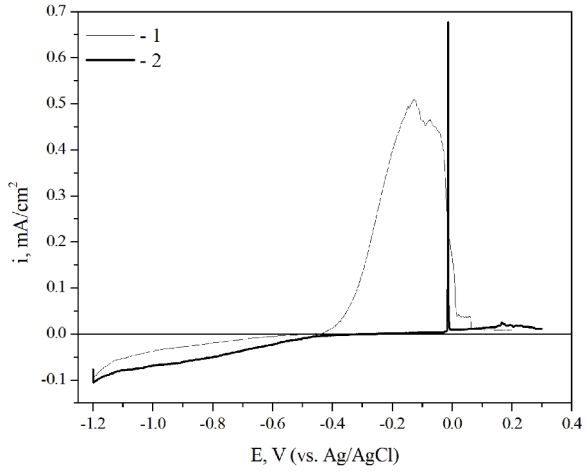

Fig. 5. Polarization curves of the alloys under study: 1 – Zr–Ti–Nb; and 2 – Ti–Al–V. The curves were recorded in a solution of 0.9 wt.% NaCl. The potential scan rate was 0.001 V/s

Photographs of the fracture surface of the Zr–Ti–Nb sample are presented in Fig. 8.

The surface of the alloy after the tensile test had a cup-shaped shape typical of a ductile fracture, with a fibrous middle part (Fig. 8,a) and a smoother conical outer surface (bevel). The width of the conical part, which was formed by the mechanism of viscous failure, characterizes the ability of the material to undergo plastic deformation and it is equal to 0.1–0.3 mm. The Zr–Ti–Nb alloy has sufficient strength and plastic deformation (Table 5), which, along with a low modulus of elasticity, allows considering this material as one of the best for use in the manufacture of implants.

One of the important characteristics of the alloy is microhardness, that is, the ability of the surface of the material to resist deformation. Figures 9 and 10 show photographs of microhardness measurements of alloys by using two different measuring devices.

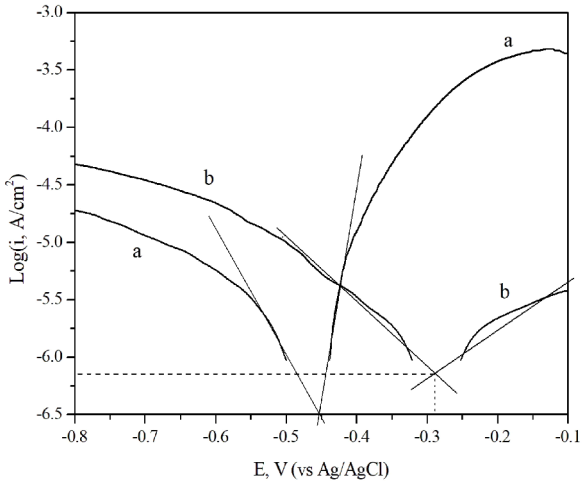

Fig. 6. Corrosion diagrams of the alloys under study: 1 – Zr–Ti–Nb; and 2 – Ti–Al–V. The curves were recorded in a solution of 0.9 wt.% NaCl. The potential scan rate was 0.001 V/s

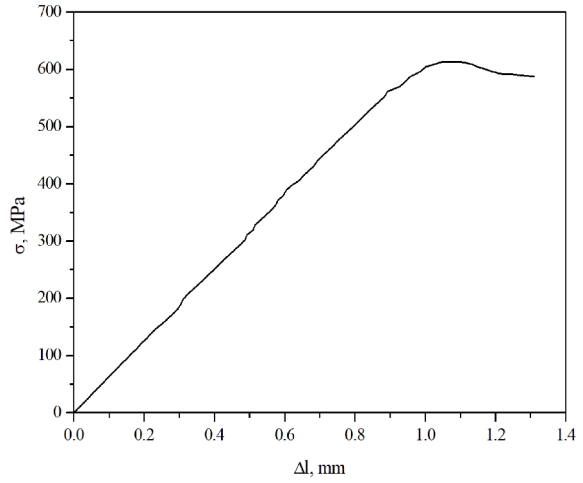

Fig. 7. Experimental tensile diagrams of the Zr–Ti–Nb alloy

Table 4

Comparison of physical properties of alloys

Alloy	Value of physical properties		
	Density, g/cm^3	Reflectivity, relative units	Electrical resistance $\times 10^6$, ohm·m
Zr–Ti–Nb	6.178±0.359	42	15.42
Ti–Al–V	4.353±0.141	39	16.56

Table 5

Comparison of mechanical properties of alloys

Alloy	Values of the mechanical properties						
	relative elongation, %	relative narrowing, %	strength limit, MPa	yield strength, MPa	modulus of elasticity, E, GPa	microhardness, H, MPa	HV, relative units
Zr–Ti–Nb	15	54	631	530	26,44	2277(±4%)	217±4.6%
Ti–Al–V	7	20	939* 900–1200 [15]	887* 800–1100 [15]	110–140 [15]	3106(±2%)	312±3.2%* 300–400 [15]

Note: * – measured values.

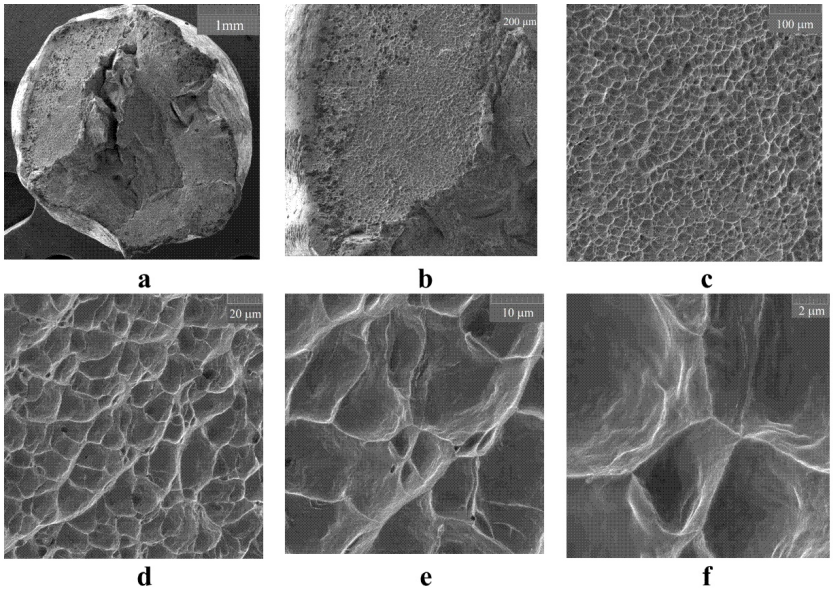

Fig. 8. SEM images of the surface of the Zr–Ti–Nb alloy sample after rupture at different magnifications

The value of microhardness for the Ti–Al–V alloy is higher by 30–36% with both measuring tools. However, both methods showed that the surface of the Ti–Al–V alloy has significantly less plasticity, which is indicated by fracture waves in places where the material is deformed by the pyramid of the measuring device, this leads to the formation of cracks and destruction surface of the product when loaded (Fig. 9,b and Fig. 10,b). Perhaps, it is because the zones of Ti–Al–V alloy are not located evenly along the surface (Fig. 3,b). This phenomenon is extremely undesirable, especially when using the Ti–Al–V alloy as a material for the manufacture of dental implants, where cracks in the coating can lead to the accumulation of bacteria and poor implantation of the implant.

Mechanical characteristics given in Table 5 indicate that the Ti–Al–V alloy has greater strength. Values of relative elongation and narrowing are greater for the Zr–Ti–Nb alloy, which indicates its significantly greater plasticity.

Conclusions

The Zr–Ti–Nb alloy does not contain toxic elements such as aluminum and vanadium. The structure and phase composition of the Zr–Ti–Nb alloy indicates a uniform arrangement of elements in the volume of the alloy.

The wetting angle of the Zr–Ti–Nb alloy with an oxide layer is significantly smaller than that of the Ti–Al–V alloy, which indicates its greater hydrophilicity and may have a positive effect on the osseointegration process.

The corrosion resistance of the Zr–Ti–Nb alloy is quite high, but lower than that of Ti–Al–V. Anodic treatment of the Zr–Ti–Nb alloy surface, leading to the formation of a passive film, can further improve the corrosion resistance of the alloy.

The Zr–Ti–Nb alloy differs slightly in physical properties from the Ti–Al–V alloy (except for density).

The Ti-Al-V alloy has significantly higher mechanical strength parameters, but the Zr–Ti–Nb alloy has significantly better properties in terms of

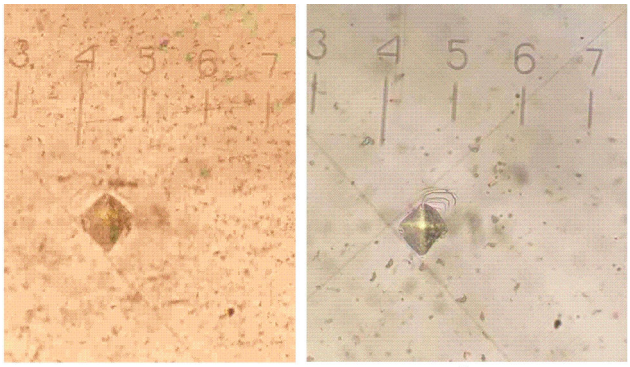

a b

Fig. 9. Photographs of the surface of a sample with an impress from a diamond pyramid for determining microhardness using the PMT-3 device: a – Zr–Ti–Nb; and b – Ti–Al–V. The scale unit corresponds to a size of 30 μm

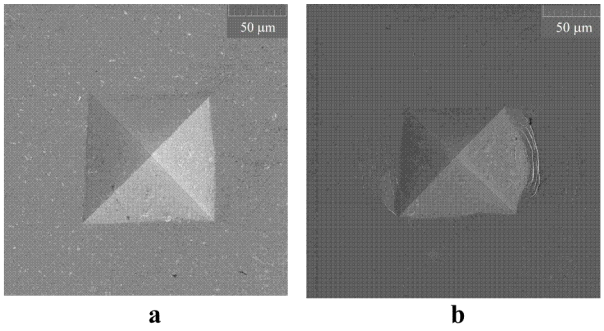

a b

Fig. 10. Photographs of the surface of a sample with an impress from a diamond pyramid for determining Vickers hardness: a – Zr–Ti–Nb; and b – Ti–Al–V.

plastic deformation compared to the Ti–Al–V alloy, as indicated by fracture and microhardness studies. It should be especially noted that the modulus of elasticity of the Zr–Ti–Nb alloy is 26.4 GPa, which is similar to the modulus of elasticity of cortical bone, unlike Ti–Al–V, whose modulus of elasticity is 110–140 GPa.

Corrosion resistance, non-toxic chemical composition, hydrophilicity and excellent mechanical properties allow recommending the Zr–Ti–Nb alloy for medical applications.

Funding

The authors are grateful to the Ministry of Education and Science of Ukraine for funding the work (project No. 0123U102008).

REFERENCES

1. *Kim I.H., Kwon T.Y., Kim K.H.* Wetting behavior of dental implants // Wetting and Wettability. – IntechOpen, 2015. – P.253-270.

2. *Enhancement* of the biocompatibility by surface nitriding of a low-modulus titanium alloy for dental implant applications / Bedouin Y., Gordin D.M., Pellen-Mussi P., Perez F., Tricot-Doleux S., Vasilescu C., Drob S.I., Chauvel-Lebret D., Gloriant T. // J. Biomed. Mater. Res. B Appl. Biomater. – 2019. – Vol.107. – No. 5. – P.1483-1490.

3. *Abdel-Hady Gepreel M., Niinomi M.* Biocompatibility of Ti-alloys for long-term implantation // J. Mech. Behav. Biomed. Mater. – 2013. – Vol.20. – P.407-415.

4. *Titanium* for orthopedic applications: an overview of surface modification to improve biocompatibility and prevent bacterial biofilm formation / Quinn J., McFadden R., Chan C., Carson L. // iScience. – 2020. – Vol.23. – Art. No. 101745.

5. *Huiskes R., Weinans H., Rietbergen B.* The relationship between stress shielding and bone resorption around total hip stems and the effects of flexible materials // Clin. Orthop. Relat. Res. – 1992. – Vol.274. – P.124-134.

6. *Kanapaakala G., Subramani V.* A review on β-Ti alloys for biomedical applications: the influence of alloy composition and thermomechanical processing on mechanical properties, phase composition, and microstructure // Proc. Inst. Mech. Eng. Pt L. – J. Mater. Des. Appl. – 2022. – Vol.237. – No. 6. – P.1251-1294.

7. *Niinomi M.* Mechanical properties of biomedical titanium alloys // Mater. Sci. Eng. A. – 1998. – Vol.243. – No. 1-2. – P.231-236.

8. *Breaking* the limit of Young's modulus in low-cost Ti–Nb–Zr alloy for biomedical implant applications / Lee T., Lee S., Kim I.S., Moon Y.H., Kim H.S., Park C.H. // J. Alloys Compd. – 2020. – Vol.828. – Art. No. 154401.

9. *Cytocompatibility* assessment of Ti-Zr-Pd-Si-(Nb) alloys with low Young's modulus, increased hardness, and enhanced osteoblast differentiation for biomedical applications / Blanquer A., Musilkova J., Barrios L., Ibanez E., Vandrovcova M., Pellicer E., Sort J., Bacakova L., Nogues C. // J. Biomed. Mater. Res. B. Appl. Biomater. – 2018. – Vol.106. – No. 2. – P.834-842.

10. *On the role* of Nb-related sites of an oxidized β-TiNb alloy surface in its interaction with osteoblast-like MG-63 cells / Jirka I., Vandrovcova M., Frank O., Tolde Z., Plsek J., Luxbacher T., Bacakova L., Stary V. // Mater. Sci. Eng. C. Mater. Biol. Appl. – 2013. – Vol.33. – No. 3. – P.1636-1645.

11. *Antibacterial* Ti-35Nb-7Zr-xCu alloy with excellent mechanical properties generated with a spark plasma sintering method for biological applications / Yi C.B., Yuan Y.X., Zhang L., Jiang Y.H., He Z.Y. // J. Alloys Compd. – 2021. – Vol.879. – Art. No. 160473.

12. *New* Zr-Ti-Nb alloy for medical application: development, chemical and mechanical properties, and biocompatibility / Mishchenko O., Ovchynnykov O., Kapustian O., Pogorielov M. // Materials. – 2020. – Vol.13. – No. 6. – Art. No. 1306.

13. *Copper* electrodeposition under a weak magnetic field: effect on the texturing and properties of the deposits / Kovalyov S.V., Girin O.B., Debiemme-Chouvy C., Mishchenko V.I. // J. Appl. Electrochem. – 2021. – Vol.51. – No. 11. – P.235-243.

14. *Influence* of weak magnetic field on electrodeposition and properties of copper films / Kovalyov S.V., Debiemme-Chouvy C., Koval'ova N.V. // Surf. Eng. Appl. Electroch. – 2021. – Vol.57. – No. 3. – P.308-314.

15. *Structure* and properties of titanium and titanium alloys / Peters M., Hemptenmacher J., Kumpfert J., Leyens C. // Titanium and titanium alloys: fundamentals and applications. – Weinheim: Wiley VCH, 2003. – P.1-36.

Received 08.07.2024

ВЛАСТИВОСТІ СПЛАВІВ Zr–Ti–Nb ТА Ti–Al–V

С.В. Ковальов, О.В. Овчинников, К.М. Сухий, В.С. Єфанов, О.О. Калініченко, Н.В. Ковальова

Стаття присвячена вивченню властивостей нового сплаву Zr-Ti-Nb та його порівнянню з відомим сплавом Ti–Al–V (ВТ-6 – аналог Grade 5). Визначено хімічний склад сплавів і стійкість до корозії. Сплав Zr–Ti–Nb не містить токсичних домішок, які є в сплаві Ti–Al–V, а саме алюміній і ванадій. Проведено структурні дослідження фаз (рентгеноструктурний аналіз) та визначено їх склад за допомогою скануючої електронної мікроскопії. Мікроструктура і фазовий склад сплаву Zr–Ti–Nb свідчить про рівномірне розташування елементів в об'ємі сплаву. Кут змочування сплаву Zr–Ti–Nb з оксидним шаром значно менший, ніж у сплаву Ti–Al–V, що свідчить про його більшу гідрофільність. Фізичні методи дослідження включали визначення густини, відбивної здатності та електропровідності. Механічні властивості досліджували шляхом визначення модуля пружності сплавів, межі міцності, межі текучості, подовжнього подовження, поперечного звуження та мікротвердості. Особливо слід зазначити, що модуль пружності сплаву Zr–Ti–Nb становить 26,4 ГПа, що аналогічно модулю пружності кортикальної кістки, на відміну від сплаву Ti–Al–V, модуль пружності якого становить 110–140 ГПа. Отримані дані свідчать про кращі хіміко-механічні властивості сплаву Zr–Ti–Nb, що дозволяє рекомендувати його для медичного застосування.

Ключові слова: біомедичний сплав, Zr–Ti–Nb; Ti–Al–V, корозія, змочуваність, хімічні, структурні та механічні властивості.

PROPERTIES OF Zr–Ti–Nb AND Ti–Al–V ALLOYS

S.V. Kovalyov* *, *O.V. Ovchynnykov, K.M. Sukhyy, V.S. Yefanov, O.O. Kalinichenko, N.V. Koval'ova

Ukrainian State University of Science and Technologies, Dnipro, Ukraine

* **e-mail: sv_kovalyov@i.ua**

This article is devoted to studying the properties of the new Zr–Ti–Nb alloy and comparing it with the well-known Ti–Al–V alloy (BT-6, Grade 5 analog). The properties were analyzed through chemical composition determination and corrosion resistance assessment. The Zr–Ti–Nb alloy does not contain the toxic impurities present in the Ti–Al–V alloy, specifically aluminum and vanadium. Structural studies were conducted to identify the phases (X-ray diffraction analysis) and their composition using scanning electron microscopy. The microstructure and phase composition of the Zr–Ti–Nb alloy indicated a uniform distribution of elements throughout the alloy. The wetting angle of the Zr–Ti–Nb alloy with an oxide layer is significantly smaller than that of the Ti–Al–V alloy, suggesting greater hydrophilicity. Physical research methods included determining density, reflectivity, and electrical conductivity. Mechanical properties were examined by determining the elastic modulus, strength limit, yield strength, longitudinal elongation, transverse contraction, and microhardness. Notably, the elastic modulus of the Zr–Ti–Nb alloy is 26.4 GPa, similar to that of cortical bone, in contrast to the Ti–Al–V alloy, which has an elastic modulus of 110–140 GPa. The obtained data indicate that the superior chemical and mechanical properties of the Zr–Ti–Nb alloy make it suitable for medical applications.

Keywords: biomedical alloy; Zr–Ti–Nb; Ti–Al–V; corrosion; wettability; chemical, structural, and mechanical properties.

REFERENCES

1. Kim IH, Kwon TY, Kim KH. Wetting behavior of dental implants. IntechOpen; 2015. p. 253-270. doi: 10.5772/61098.

2. Bedouin Y, Gordin DM, Pellen-Mussi P, Perez F, Tricot-Doleux S, Vasilescu C, et al. Enhancement of the biocompatibility by surface nitriding of a low-modulus titanium alloy for dental implant applications. *J Biomed Mater Res B Appl Biomater.* 2019; 107(5): 1483-1490. doi: 10.1002/jbm.b.34240.

3. Abdel-Hady Gepreel M, Niinomi M. Biocompatibility of Ti-alloys for long-term implantation. *J Mech Behav Biomed Mater.* 2013; 20: 407-415. doi: 10.1016/j.jmbbm.2012.11.014.

4. Quinn J, McFadden R, Chan CW, Carson L. Titanium for orthopedic applications: an overview of surface modification to improve biocompatibility and prevent bacterial biofilm formation. *iScience.* 2020; 23: 101745. doi: 10.1016/j.isci.2020.101745.

5. Huiskes R, Weinans H, van Rietbergen B. The relationship between stress shielding and bone resorption around total hip stems and the effects of flexible materials. *Clin Orthop Relat Res.* 1992; 274: 124-134.

6. Kanapaakala G, Subramani V. A review on β-Ti alloys for biomedical applications: the influence of alloy composition and thermomechanical processing on mechanical properties, phase composition, and microstructure. *Proc Inst Mech Eng Pt L J Mater Des Appl.* 2022; 237(6): 1251-1294. doi: 10.1177/14644207221141768.

7. Niinomi M. Mechanical properties of biomedical titanium alloys. *Mater Sci Eng A*. 1998; 243: 231-236. doi: 10.1016/S0921-5093(97)00806-X.

8. Lee T, Lee S, Kim IS, Moon YH, Kim HS, Park CH. Breaking the limit of Young's modulus in low-cost Ti–Nb–Zr alloy for biomedical implant applications. *J Alloys Compd*. 2020; 828: 154401. doi: 10.1016/j.jallcom.2020.154401.

9. Blanquer A, Musilkova J, Barrios L, Ibanez E, Vandrovcova M, Pellicer E, et al. Cytocompatibility assessment of Ti-Zr-Pd-Si-(Nb) alloys with low Young's modulus, increased hardness, and enhanced osteoblast differentiation for biomedical applications. *J Biomed Mater Res B Appl Biomater*. 2018; 106: 834-842. doi: 10.1002/jbm.b.33892.

10. Jirka I, Vandrovcova M, Frank O, Tolde Z, Plsek J, Luxbacher T, et al. On the role of Nb-related sites of an oxidized β-TiNb alloy surface in its interaction with osteoblast-like MG-63 cells. *Mater Sci Eng C Mater Biol Appl*. 2013; 33(3): 1636-1645. doi: 10.1016/j.msec.2012.12.073.

11. Yi CB, Yuan YX, Zhang L, Jiang YH, He ZY. Antibacterial Ti-35Nb-7Zr-xCu alloy with excellent mechanical properties generated with a spark plasma sintering method for biological applications. *J Alloys Compd*. 2021; 879: 160473. doi: 10.1016/j.jallcom.2021.160473.

12. Mishchenko O, Ovchynnykov O, Kapustian O, Pogorielov M. New Zr-Ti-Nb alloy for medical application: development, chemical and mechanical properties, and biocompatibility. *Materials*. 2020; 13(6): 1306. doi: 10.3390/ma13061306.

13. Kovalyov SV, Girin OB, Debiemme-Chouvy C, Mishchenko VI. Copper electrodeposition under a weak magnetic field: effect on the texturing and properties of the deposits. *J Appl Electrochem*. 2021; 51: 235-243. doi: 10.1007/s10800-020-01492-3.

14. Kovalyov SV, Debiemme-Chouvy C, Koval'ova NV. Influence of weak magnetic field on electrodeposition and properties of copper films. *Surf Eng Appl Electrochem*. 2021; 57: 308-314. doi: 10.3103/S1068375521030091.

15. Peters M, Hemptenmacher J, Kumpfert J, Leyens C. Structure and properties of titanium and titanium alloys. In: Leyens C, Peters M, editors. *Titanium and titanium alloys: fundamentals and applications*. Weinheim: Wiley VCH; 2003. p.1-36. doi: 10.1002/3527602119.ch1.